

# Preparation of Chitosan-Bound Nitrobenzaldehyde Metal Complexes and Studies on Its Catalytic Oxidative Activity and Reactive Mechanism

YUE CHANG,<sup>1,2</sup> YUNPU WANG,<sup>2</sup> ZHIXING SU<sup>1</sup>

<sup>1</sup> Department of Chemistry, Lanzhou University, Lanzhou 730000, China

<sup>2</sup> Department of Chemistry, Northwest Normal University, Lanzhou 730070, China

Received 16 December 2000; accepted 8 May 2001

**ABSTRACT:** Chitosan-bound nitrobenzaldehyde metal complexes (*m*-CNBDM and *o*-CNBDM, where M is Mn or Ni) were prepared and characterized by infrared, X-ray photoelectron spectroscopy, solid-state <sup>13</sup>C-NMR cross-polarity/magic-angle spinning, inductively coupled plasma, and elemental analysis. The complexes were found to be catalysts for the oxidation of hydrocarbons with molecular oxygen under mild conditions. *o*-CNBDNi has a certain catalytic activity in the oxidation of *n*-propylbenzene and isopropylbenzene and has no activity in the oxidation of ethylbenzene. Both *o*-CNBDMn and *m*-CNBDNi catalyze the oxidation of all the aforementioned hydrocarbons, whereas *m*-CNBDMn has no catalytic activity. The main oxidative products of ethylbenzene and *n*-propylbenzene are the same as  $\alpha$ -ol and  $\alpha$ -one, but they are 2-benzyl-isopropynol and isopropylbenzene peroxide for isopropylbenzene. A mechanism for the catalytic oxidative process is proposed. © 2002 John Wiley & Sons, Inc. *J Appl Polym Sci* 83: 2188–2194, 2002

**Key words:** chitosan; chitosan-bound complexes; catalytic oxidation; mechanism; catalysts; alkylbenzene; oxygen

## INTRODUCTION

Chitosan, which is easily obtained by the alkaline deacetylation of chitin, one of the most abundant organic materials (chitin extensively exists in the shells of crabs and shrimp, insects, and molds), has both hydroxyl and amine groups that can be modified. It has been applied to the treatment of wastewater,<sup>1,2</sup> membrane materials,<sup>3,4</sup> medicines,<sup>5–9</sup> printing and dyeing,<sup>10,11</sup> cosmetics,<sup>12</sup> foods,<sup>13</sup> and so forth. It has also been applied as a supporter of active Pd used in catalytic hydrogenation in the oil industry because it is easily

separated from the products and recycled by activation.<sup>14</sup> However, applications of chitosan as a natural polymer supporter in the selective catalytic oxidation of hydrocarbons, a current topic of research,<sup>15–18</sup> are still sparse. Therefore, in this study, different chitosan-bound nitrobenzaldehyde metal complexes were prepared and characterized. The behavior of the catalytic activity in the oxidation of hydrocarbons with molecular oxygen is reported, and a mechanism for catalytic oxidation is proposed.

## EXPERIMENTAL

### Materials and Equipment

Chitin and other reagents were obtained commercially. Ethylbenzene, *n*-propylbenzene, and isopropylbenzene were purified before use.

Correspondence to: Z. Su (suzx@lzu.edu.cn).

*Journal of Applied Polymer Science*, Vol. 83, 2188–2194 (2002)  
© 2002 John Wiley & Sons, Inc.  
DOI 10.1002/app.10183

Infrared (IR) spectra were recorded in KBr on an Alpha-Centauri Fourier transform infrared (FTIR) spectrophotometer (Shimadzu, Japan). Small-area X-ray photoelectron spectroscopy (XPS) data were recorded with a PHI-5702 multitechnique system (PHI, U.S.A.); the power source was a Mg K $\alpha$  line, and the Ag<sub>3d5/2</sub> full width at half-maximum was less than or equal to 0.48 eV. Elemental analysis was performed on an Itali Carbo-Erba 1106 elemental autoanalyzer (Carbo-Erba, Italy). The metal content was obtained with an ARL-3520 inductively coupled plasma (ICP) instrument (TJA, U.S.A.). The products of oxidation were detected and analyzed with a GC-16A gas chromatograph (Shimadzu), a QP-1000A gas chromatography/mass spectrometry (GC/MS) system (Shimadzu), and a gas chromatography/infrared (GC/IR) system (HP 5890II GC and Bio-Rad 65A FtS IR system, Hewlett-Packard, U.S.A.). The solid-state <sup>13</sup>C-NMR spectra for complexes were recorded on a Unity 400-MHz NMR spectrometer (Bruker, Switzerland).

#### Synthesis of Chitosan-Bound *o*-Nitrobenzaldehyde Nickel Complexes (*o*-CNBDNi)

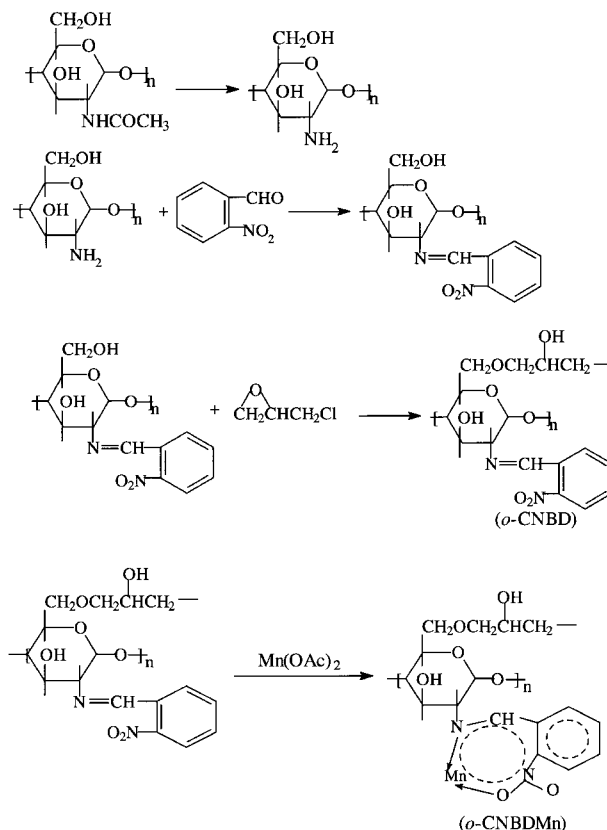
Chitosan was prepared, and its amido content was determined by a method described in the literature.<sup>19,20</sup>

The synthesis of chitosan-bound nitrobenzaldehyde followed ref. 21: a solution of chitosan (0.023 mol, 3.75 g) and *o*-nitrobenzaldehyde (0.046 mol, 7 g) in benzene (20 mL) was stirred for 18 h near reflux and then was filtered at the room temperature. A yellow solid from this process was added to a solution of epoxychloropropane (2.2 g, 0.023 mol) and sodium hydroxide (4 g, 0.1 mol) in dichloroethane (40 mL). After stirring at 313 K for about 10 h, the mixture was filtered, and the solid was washed repeatedly with water until the pH of the washing solution was 7. With drying *in vacuo*, a yellow product of chitosan-bound *o*-nitrobenzaldehyde (*o*-CNBD) was obtained.

A mixture of *o*-CNBD (0.7 g) and NiCl<sub>2</sub> · 6H<sub>2</sub>O (3.2 g) in anhydrous ethanol (40 mL) was refluxed for about 10 h with stirring and was then cooled to room temperature. The green chelate *o*-CNBDNi was filtered, washed thoroughly with ethanol, and dried *in vacuo*.

Chitosan-bound *m*-nitrobenzaldehyde (*m*-CNBD) and corresponding metal complexes (*m*-CNBDMn and *m*-CNBDNi) were prepared with the same method.

The synthesis route is shown in Scheme 1.



Scheme 1

The elemental contents (as analyzed with the elemental autoanalyzer) were as follows: C, 42.01%, H, 6.92%, and N, 8.30% in *m*-CNBD and C, 41.64%, H, 7.31%, and N, 8.06% in *o*-CNBD.

#### Oxidation of Hydrocarbons

Catalyst and hydrocarbon were added to a glass flask with a gas inlet tube connected to a gas burette and an oxygen storage bottle and a gas outlet tube that could be opened to the air. The mixture was heated in an oil bath and stirred with a magnetic stirrer. The volume of oxygen consumed was measured from the burette.

## RESULTS AND DISCUSSION

#### Characterization

The metal contents analyzed with a model ARL-3520 ICP atomic emission spectrometer and IR spectra obtained on an Alpha-Centauri FTIR spectrophotometer (KBr disks) are shown in Table I. With respect to chitosan, a new peak ap-

**Table I ICP and IR Spectra Data of Complexes**

Complex	Metal Content (%)	Wavelength (cm <sup>-1</sup> )			
		$\nu_{\text{C}=\text{N}}$	$\nu_{\text{C}=\text{C}}$	$\nu_{\text{O}-\text{M}}$	$\nu_{\text{N}-\text{M}}$
<i>m</i> -CNBD	—	1654	1601/1458	—	—
<i>m</i> -CNBDNi	1.91	1624	1607/1458	403	351
<i>m</i> -CNBDMn	1.98	1631	1602/1459	435	362
<i>o</i> -CNBD	—	1632	1606/1457	—	—
<i>o</i> -CNBDNi	0.56	1613	1627/1459	420	326
<i>o</i> -CNBDMn	1.69	1618	1627/1462	428	357

pears at 1654 cm<sup>-1</sup> in *o*-CNBD, and 1632 cm<sup>-1</sup> in *m*-CNBD is the stretching vibration absorption peak of the C=N band. Combined with the characteristic absorption of  $\nu_{\text{C}=\text{C}}$  of the benzene ring at about 1600 and 1458 cm<sup>-1</sup>, it indicates that nitrobenzaldehyde is chitosan-bonded. The absorption at 435 and 362 cm<sup>-1</sup>, attributed to  $\nu_{\text{O}-\text{Mn}}$  and  $\nu_{\text{N}-\text{Mn}}$  in *m*-CNBDMn, or the absorption at 403 and 351 cm<sup>-1</sup>, due to  $\nu_{\text{O}-\text{Ni}}$  and  $\nu_{\text{N}-\text{Ni}}$  in *m*-CNBDNi, shows the oxygen and nitrogen atoms in *m*-CNBD coordinating with metal ions (the same conclusion can be drawn from an analysis of the spectra of other complexes). The blue-shift of  $\nu_{\text{C}=\text{N}}$  in metal complexes (compared with chitosan-bound nitrobenzaldehyde) can also indicate the coordination property of nitrogen.

To confirm the coordination of chitosan-bound nitrobenzaldehyde with metal ions, we measured small-area XPS data of chitosan, *o*-CNBD, manganese oxalate (Mn(OAc)<sub>2</sub>), and *o*-CNBDMn, and the results, fitted with a computer fitting program, are listed in Table II. The binding energy of C<sub>1s1/2</sub>, due to C—H, has a slight decrease, whereas the binding energy of C<sub>1s1/2</sub>, due to C—O in *o*-CNBD, has a change of -0.63 eV compared with that of chitosan, which indicates the binding of ep-

oxychloropropane to chitosan, and it only increases 0.28 eV compared with that of *o*-CNBDMn. The binding energy of C<sub>1s1/2</sub>, due to C—N in *o*-CNBD, has a very small change compared with that of chitosan, whereas it increases 1.03 eV when *o*-CNBDMn is formed. The binding energy of N<sub>1s1/2</sub> in chitosan is 398.89 eV; when *o*-nitrobenzaldehyde links to chitosan, it changes to 398.08 eV because of the nitrogen atom combining with the carbon atom in *o*-nitrobenzaldehyde. Following the same analysis, we find that the binding energies of O<sub>1s1/2</sub> and N<sub>1s1/2</sub>, due to O—N and N—C, respectively, in *o*-CNBDMn apparently increase compared with that in *o*-CNBD. The Mn<sub>2p3/2</sub> binding energy increases 1.7 eV after Mn(OAc)<sub>2</sub> · 2H<sub>2</sub>O reacts with *o*-CNBD.

When metal complexes are formed, although only oxygen and nitrogen atoms combine with metal ions, the electron cloud distributes evenly in the chelating cycle, inducing changes in the binding energies of other elements and the shifting of the absorption peak.

This analysis can be verified by the measurement of solid-state <sup>13</sup>C-NMR spectra of *o*-CNBD and *o*-CNBDMn (Fig. 1). The signal assigned to the carbon of the C=N group of *o*-CNBD at 120.6 ppm apparently decreases when complexes of *o*-

**Table II XPS Data of Corresponding Substances**

Substance	Binding Energy (eV)							
	C <sub>1s1/2</sub>			O <sub>1s1/2</sub>		N <sub>1s1/2</sub>		Mn <sub>2p3/2</sub>
	H—C	O—C	N—C	H—O	N—O	C—N	O—N	
Chitosan	284.61	286.12	286.66	532.31	—	398.89 <sup>a</sup>	—	—
<i>o</i> -CNBD	284.57	285.49	286.53	531.50	530.61	398.08	399.19	—
<i>o</i> -CNBDMn	284.50	285.77	287.56	531.07	532.21	398.62	399.76	642.12
Mn(OAc) <sub>2</sub>	—	—	—	—	—	—	—	640.42

<sup>a</sup> Binding energy of N<sub>1s1/2</sub> in N—H.

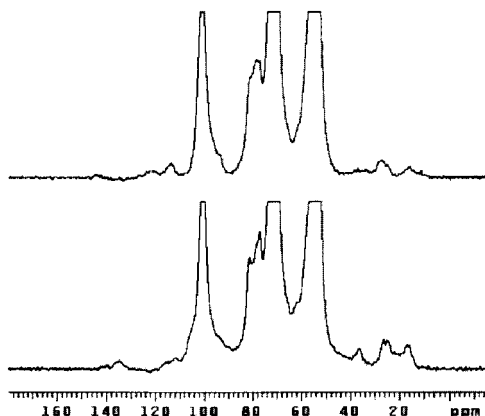


**Figure 1** Solid-state  $^{13}\text{C}$ -NMR spectra of *o*-CNBD (top) and *o*-CNBDMn (bottom).

CNBDMn form. Because of the effect of the electron attraction of manganese, it shifts to 134.8 ppm. The signal at 113.6 ppm, assigned to the carbon of the benzene ring, also decreases when metal complexes form, mostly because of the redistribution of the electron cloud. The signal at 100.7 ppm is the binding peak of glycoside of polysaccharose. Also, the signals at 82.3, 77.0, 71.2, and 52.9 ppm are the characteristic peaks of polysaccharose. The signals of carbons of methyl groups linked to oxygen and not linked to oxygen appear at 36.2, 26.3, 24.8, and 16.7 ppm, respectively. Because of the change in the chemical circumstances, the shape of the carbons has a certain variance.

Having combined our analyses of the IR spectra, XPS, and solid-state  $^{13}\text{C}$ -NMR, we propose the structure of *o*-CNBDMn given in Scheme 1.

### Catalytic Activity of Different Metal Complexes

The properties of all the complexes as catalysts in the oxidation of ethylbenzene, *n*-propylbenzene, and isopropylbenzene in the presence of molecular oxygen were determined. Although *m*-CNBDMn has no catalytic activity in the oxidation of the three substrates and *o*-CNBDNi has no catalytic activity in the oxidation of ethylbenzene, the experiments show that all the other complexes have a certain catalytic activity. Figure 2 shows the volume of oxygen consumption versus time in the presence of different complexes and different substrates. Generally, in contrast to the complexes of nickel, the complexes of manganese have longer induction periods and lower rates of oxygen consumption. Under the experimental conditions, although the rate of oxygen consumption in the oxidation of *n*-propyl-

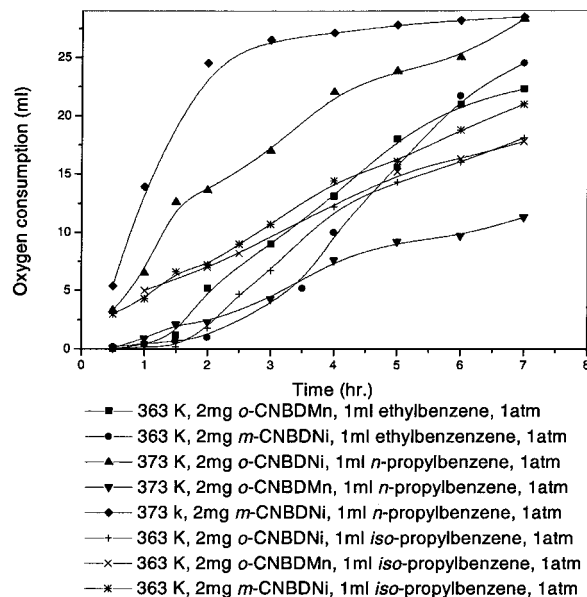
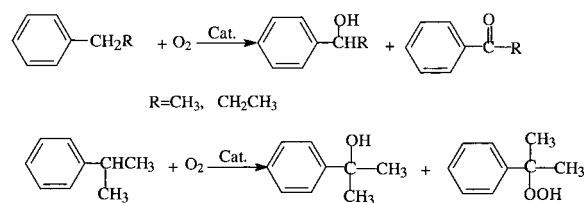


**Figure 2** Curves of oxygen consumption versus time.

benzene in the presence of *m*-CNBDNi at the beginning stage is highest, after a reaction time exceeding about 2 h, it changes slowly, whereas others change quickly, especially for the *m*-CNBDNi/ethylbenzene system. The oxidation products measured by GC/MS and GC/IR show that the oxidation of ethylbenzene and *n*-propylbenzene both occur in the  $\alpha$ -carbon linked with the benzene ring to form mainly  $\alpha$ -ol and  $\alpha$ -one (ethylbenzene forms 1-phenyl ethanol and acetophenone, and *n*-propylbenzene forms 1-phenyl propanol and ethylphenylketone; see Scheme 2). When isopropylbenzene is oxidized by molecular oxygen in the presence of those complexes, 2-benzyl-isopropynol (PP) and isopropylbenzene peroxide (CHP) are predominantly formed (also see Scheme 2). The result is different from that of the oxidation reported in the literature.<sup>16</sup> The conversion of substrates and corresponding products and the selectivity are listed in Table III. Under the same conditions, the conversion of ethylbenzene in the presence of *m*-CNBDNi is slightly higher than that in the presence of *o*-CNBDMn,



**Scheme 2**

**Table III** Oxidation Properties of Hydrocarbon Under Different Catalysts

Catalyst	Ethylbenzene			<i>n</i> -Propylbenzene			isoPropylbenzene		
	Conversion (%)	Selectivity (%)		Conversion (%)	Selectivity (%)		Conversion (%)	Selectivity (%)	
		$\alpha$ -ol	$\alpha$ -one		$\alpha$ -ol	$\alpha$ -one		PP	CHP
<i>o</i> -CNBDMn	12.2	34.4	41.1	7.0	14.9	35.3	17.2	53.1	42.5
<i>m</i> -CNBDNi	13.4	41.8	31.4	17.7	19.9	64.9	13.0	34.8	56.1
<i>o</i> -CNBDNi	0.0	0.0	0.0	17.3	15.3	69.8	11.2	51.0	47.2

Substrate = 1 mL, catalyst = 2 mg, temperature = 363 K, reaction time = 7 h.

whereas it is obviously higher in the oxidation of *n*-propylbenzene. For the oxidation of isopropylbenzene, the conversion is highest under *o*-CNBDMn, but the selectivity seems better under *m*-CNBDNi. Both *m*-CNBDNi and *o*-CNBDNi show good activity in the catalytic oxidation of *n*-propylbenzene, for which the selectivity of  $\alpha$ -one is much higher than that of  $\alpha$ -ol.

### Mechanism of Catalytic Oxidation

Most studies have proposed a free-radical chain mechanism for the process of catalytic oxidation, with molecular oxygen and metal ions playing the role of catalyzing chain initiation and the decomposition of peroxide.<sup>17,22–25</sup> Wang et al.<sup>7</sup> reported the preparation of polymer-bound benzotriazole copper complexes and studied its catalytic activity in the oxidation of ethylbenzene and cumene, where they found that the oxidation process had an induction period and that the first step was the deprotonation of the substrate, which was very

important for the oxidation. However, why there is an induction period in many catalytic oxidation processes and how deprotonation happens have not been explained. In another literature report,<sup>18</sup> the authors thought that the base played an important role in the formation of free radicals. Because no base is present in this system (experimentation also shows that the addition of base or acid can decrease the catalytic activity), so that we might explain the mechanism of catalytic oxidation, the concentrations of ethylbenzene and the oxidation products at different reaction times were measured with GC analysis. Plots of ethylbenzene conversions and yields of reacted products versus time are depicted in Figure 3. The low reactivity of the catalyst is due to the heterogeneity of the system. However, curves can supply some kinetic information for the analysis. The yield of  $\alpha$ -ol increases in the beginning, has nearly no change after 3 h of reaction, and has a decreasing tendency after reacting a longer time,

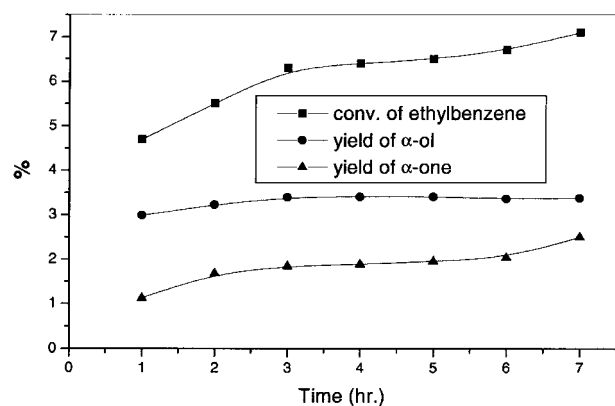


**Figure 3** Kinetic curves of ethylbenzene oxidation (substrate, 1 mL; *o*-CNBDNi, 2 mg; temperature, 363 K; pressure, 1 atm).

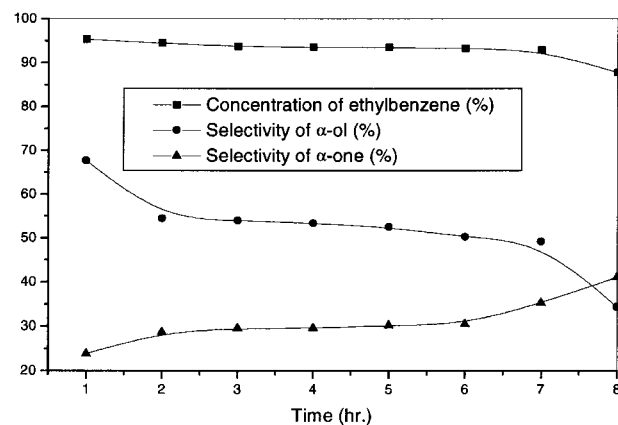


**Figure 4** Distribution of the substrate and products (substrate, 1 mL; *o*-CNBDNi, 2 mg; temperature, 363 K; pressure, 1 atm).



whereas the yield of  $\alpha$ -one increases all along. Figure 4 also shows that the selectivity of  $\alpha$ -ol decreases, whereas that of  $\alpha$ -one increases. It has been reported that 2,6-xylenol can be catalytically oxidized to tetramethyldiphenoquinone<sup>18</sup> and cyclohexanol can be oxidized to cyclohexanone<sup>26</sup> in the presence of molecular oxygen under mild conditions. This can explain the aforementioned phenomenon, the transformation of  $\alpha$ -ol to  $\alpha$ -one during the reaction process. To confirm this conclusion, we carried out an experiment in which 1-phenyl ethanol was catalytically oxidized under the same conditions.

Because the catalytic oxidation is a gas-liquid-solid phase reaction, the first step is the adsorption of gas and liquid to the catalyst and its activation. Because this system is under a pressure of 1 atm and the oxygen must penetrate the liquid and interface of different phases, be adsorbed around the surface of catalyst, and be activated, the rate of adsorption is very slow. This is why an induction period exist. Moreover, different induction periods exist because the structure and size of the catalyst also greatly influence the gas adsorption. After oxygen is adsorbed and is activated on the surface of the catalyst, the activated oxygen atom can induce the deprotonation of ethylbenzene.

The formation of peroxide is a common idea in the study of this mechanism. As soon as the free radical is produced, it is easy to form the peroxide with molecular oxygen in the presence of the catalyst. Because the rate of peroxide formation is very quick and the peroxide reacts with the sub-

strate easily and rapidly to form  $\alpha$ -ol, it cannot be detected in the reaction process. Moreover, in the presence of the catalyst,  $\alpha$ -ol is transformed to  $\alpha$ -one. Because the rate of forming  $\alpha$ -ol is higher than that of forming  $\alpha$ -one, the yield of  $\alpha$ -ol is also higher than that of  $\alpha$ -one, and this is why the yield of  $\alpha$ -one still increases but the yield of  $\alpha$ -ol remains nearly unchangeable.

On the basis of the reaction properties, it is clear that a metal must change its oxidation state in the course of the reaction and that the nature and spatial arrangement of ligands around the metal have a certain effect on the oxidation process. Therefore, a mechanism for catalytic oxidation is proposed in Scheme 3.

## CONCLUSIONS

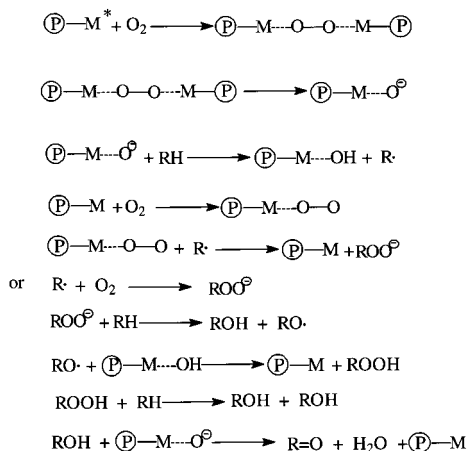
The chitosan-bound nitrobenzaldehyde metal complexes *m*-CNBDMn, *o*-CNBDMn, *m*-CNBDNi, and *o*-CNBDNi were prepared and characterized by IR, XPS, ICP, solid-state <sup>13</sup>C-NMR, and elemental analysis.

The complexes are catalysts for the oxidation of hydrocarbons with molecular oxygen under mild conditions. *o*-CNBDNi has a certain catalytic activity in the oxidation of *n*-propylbenzene and isopropylbenzene and has no activity in the oxidation of ethylbenzene. Both *o*-CNBDMn and *m*-CNBDNi can catalyze the oxidation of all the aforementioned hydrocarbons, whereas *m*-CNBDMn has no catalytic activity. The main oxidation products of ethylbenzene and *n*-propylbenzene are the same as  $\alpha$ -ol and  $\alpha$ -one, but they are PP and CHP for isopropylbenzene.

Kinetic detection shows that the selectivity of  $\alpha$ -ol decreases whereas that of  $\alpha$ -one increases during the oxidation process. The mechanism of catalytic oxidation is the substrate being oxidized with molecular oxygen to  $\alpha$ -ol and then being transformed into  $\alpha$ -one in the presence of the catalyst.

## REFERENCES

1. McKay, G.; Kelly, J. C.; Mcconvey, I. F. *Adsorpt Sci Technol* 1991, 8, 13.
2. Wada, S.; Ichikawa, H.; Tatsumi, K. *Biotechnol Bioeng* 1993, 42, 854.
3. Peter, M. G. *Plast Eng* 1995, 29, 37.
4. Li, W. J.; Zhong, W.; Zheng, W. Y.; Li, P. *Chin Sci Bull* 1991, 15, 1191.



\*  $\textcircled{P}$ : CNBD, M: metal

Scheme 3

5. Li, W. J.; Pan, W. S.; Tang, Y. *Chem J Chin Univ* 1993, 14, 135.
6. Lorenzo-Lamosa, M. L.; Remunan-Lopez, C.; Vila Jato, J. L.; Alonso, M. J. *J Controlled Release* 1998, 52, 109.
7. Saivayaanagi, Y. *Chem Pharm Bull* 1982, 30, 4213.
8. Muzzaerli, R. A. *Carbohydr Polym* 1993, 20, 7.
9. Kwweon, D.; Kang, D. W. *J Appl Polym Sci* 1999, 74, 458.
10. Jung, B. Y.; Kim, C. H.; Choi, K. S.; Moolee, Y.; Kim, J. J. *J Appl Polym Sci* 1999, 72, 1113.
11. Muzzaerli, R. A. *Carbohydr Polym* 1988, 15, 1.
12. Huang, Y. L. *Yin Ran* 1998, 24, 12.
13. Dong, Y. M.; Yuan, Y. H.; Qiu, W. B.; Wu, Y. S.; Wang, M.; Xu, C. Y. *Food Sci Technol (in Chinese)* 2000, No. 5, 28.
14. Yan, R. X. *Shuirongxing Gaofenzi; Huaxuegongye Chubanshe: Beijing*, 1998; p 554.
15. Wang, Y. P.; Chang, Y.; Wang, R. M.; Zha, F. *J Mol Catal A* 2000, 31, 159.
16. Lei, Z. Q.; Han, X. E.; Hu, Y. L.; Wang, R. M.; Wang, Y. P. *J Appl Polym Sci* 2000, 75, 1068.
17. Wang, R. M.; Chai, C. P.; He, Y. F.; Wang, Y. P.; Li, S. B. *Eur Polym J* 1999, 35, 2051.
18. Selvaraj, P. C.; Mahadevan, V. *Polymer* 1997, 39, 1741.
19. Han, H. F.; Qian, J. Q. *Huaxue Shijie* 1997, 38, 523.
20. Wang, Z. J. *Huaxue Shijie* 1986, 27, 22.
21. Liu, F.; Dong, S. H.; Xu, Y. W. *Huanjing Huaxue* 1996, 15, 207.
22. Grinstaff, M. W.; Hill, M. G.; Labinger, J. A.; Gray, H. B. *Science* 1994, 264, 311.
23. Birnbaum, E. R.; Grinstaff, M. W.; Labinger, J. A.; Bercaw, J. E.; Gray, H. B. *J Mol Catal A* 1995, 104, 119.
24. Wang, R. M.; Hao, C. J.; Wang, Y. P.; Li, S. B. *J Mol Catal A* 1999, 147, 173.
25. Wang, R. M.; Yu, T. Z.; He, Y. F.; Wang, Y. P.; Xie, B. H.; Xia, C. G.; Suo, J. Q. *Gaodeng Xuexiao Huaxue Xuebao* 1999, 20, 1772.
26. Punniyamurthy, T.; Bhatia, B.; Reddy, M. M.; Maikap, G. C. *Tetrahedron* 1997, 53, 7649.